PROCEEDINGS OF SCIENCE

Multi-Messenger Signatures of the Milky Way Galaxy in Cosmic Rays, Neutrinos, and Gamma Rays

Dmitri Semikoz[a,*]

[a] *Laboratory of Astroparticle Physics and Cosmology, CNRS, Université de Paris Cité, 75013 Paris, France*

E-mail: semikoz@apc.in2p3.fr

In this talk, I reviewed recent measurements of the local Galactic cosmic ray flux up to the knee region, as well as the emission from the Milky Way galaxy in gamma-rays and neutrinos within the same energy range. I presented an overview of both observational data and example theoretical models of multi-messenger diffuse emission from the Galaxy.

39th International Cosmic Ray Conference (ICRC2025)
15–24 July 2025
Geneva, Switzerland

ICRC 2025
The Astroparticle Physics Conference
Geneva July 15-24, 2025

*Speaker

PoS(ICRC2025)1399

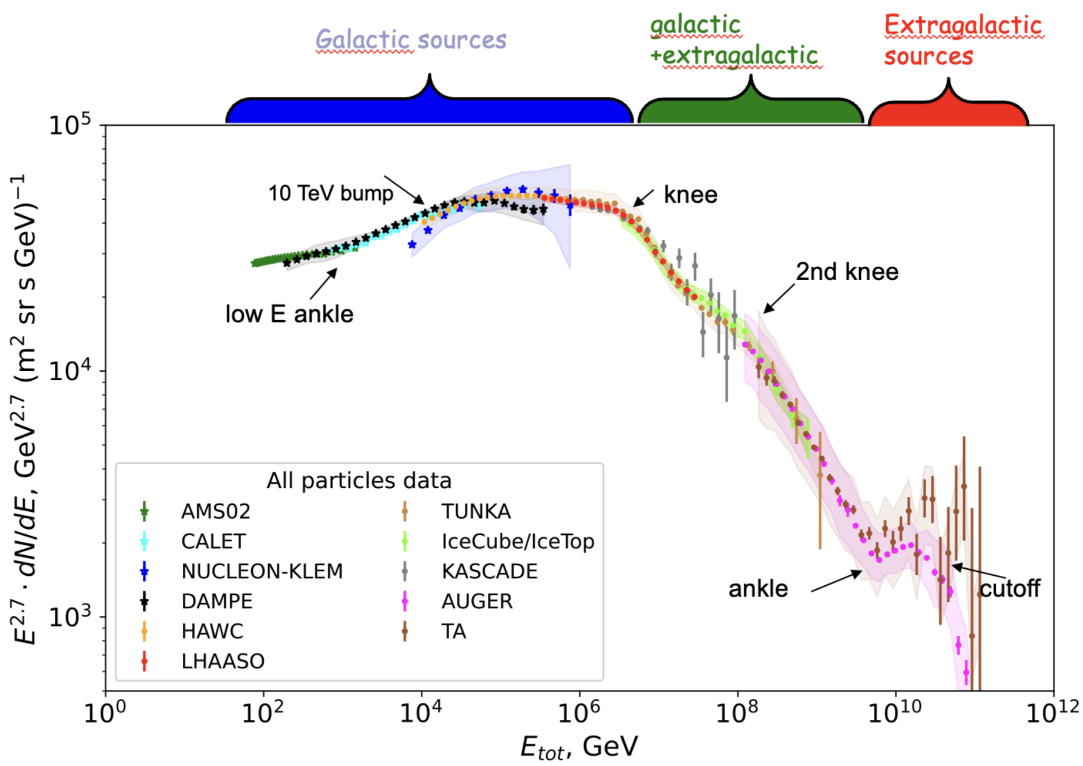

Figure 1: Cosmic ray all particle spectrum as function of energy multiplied by $E^{2.7}$. CR with energies below knee come from Galactic sources. CR with energies above ankle from extragalactic sources. In between mixed galactic and extragalactic cosmic rays.

1. Cosmic rays

Cosmic Rays (CR) are high-energy particles originating from outer space, primarily composed of protons and heavier nuclei. These particles span a wide range of energies, from a GeV up to beyond 10^{20} eV. At energies typically below 100 TeV, cosmic rays can be measured directly in space using satellite-borne experiments. These instruments are capable of identifying the charge and energy of primary cosmic rays. Currently, three major space-based experiments are at the forefront of direct cosmic ray measurements: the Alpha Magnetic Spectrometer (AMS-02) [1], the CALorimetric Electron Telescope (CALET) [2], and the DArk Matter Particle Explorer (DAMPE) [3]. These missions, operating in low Earth orbit, are designed to precisely measure the energy spectra and composition of cosmic rays, with particular focus on electrons, positrons, protons, and heavier nuclei. Those experiments see two rigidity features in the CR spectrum: low energy ankle at 300 GV and bump around 10 TV, see Fig. 1.

However, the flux of cosmic rays decreases rapidly with increasing energy, approximately following $1/E^{2.7}$ a power-law spectrum. At knee at $E = 4 * 10^{15}$ eV it steepens to $1/E^{3.1}$ a power-law spectrum and drop even faster, see Fig. 1. As a result, the number of detected events at higher energies becomes extremely low for satellites, which typically have an effective area on the order of m^2. Consequently, direct detection methods become statistically limited above energy $\sim$ 100 TeV.

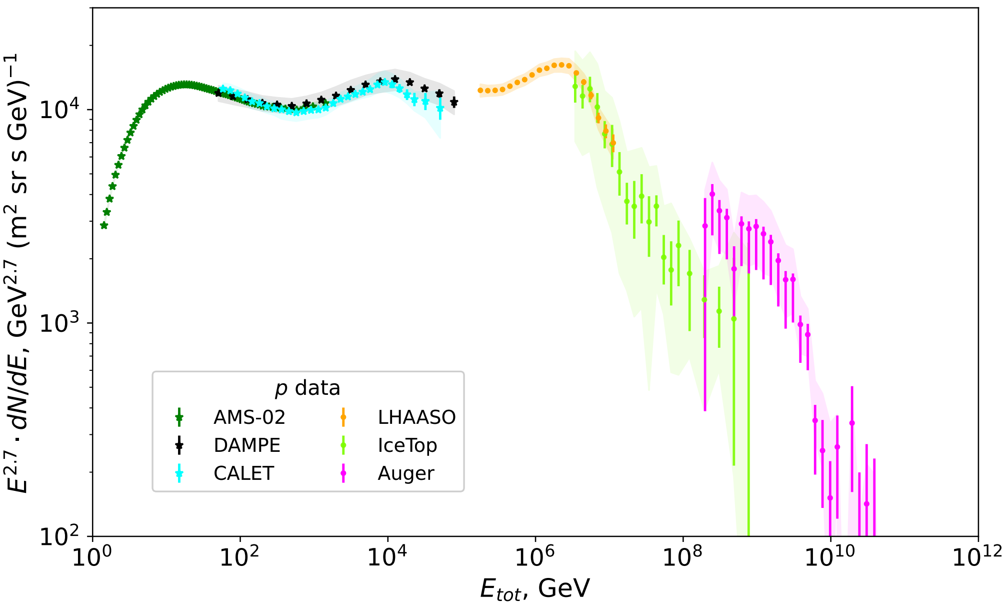

Figure 2: Cosmic ray proton spectrum measured by AMS-02 [7], DAMPE[8], CALET[9], LHAASO[10], IceCube [11] and Auger[12].

In this high-energy regime, ground-based observatories observe the extensive air showers produced when cosmic rays interact with atmospheric nuclei. Secondary particles and electromagnetic radiation generated in these cascades—such as muons, electrons, photons, Cherenkov light , fluorescent light, radio emission —are recorded to reconstruct the properties of the original cosmic rays. Ground-based detectors can cover large surface areas (from tens of thousands of square meters to thousands of square kilometres), enabling them to gather sufficient statistics even at ultra-high energies. In Fig. 1 we show CR energy spectrum measured by ground based experiments KASCADE, Icetop, TUNKA, HAWC and LHAASO in knee region and Auger and TA at highest energies. All experiments except AMS-02 does not have possibility directly calibrate their absolute energy scale. In Fig. 1 we normalised all absolute energy scales to measurements of AMS-02. Note, that change in the energy scales is within systematic uncertainty for all experiments.

Knee at $E = 4 * 10^{15}$ eV is most visible feature in the cosmic ray spectrum in Fig. 1. It was first measured in 1958 by MSU experiment [4]. Most recent measurement was done by LHAASO in ref. [5].

Spectrum has second knee $E = 10^{17}$ eV, ankle at $E = 3 * 10^{18}$ eV and cutoff at energies around $E = 10^{20}$ eV. At energies above ankle $E > 3 * 10^{18}$ eV cosmic rays are of extragalactic origin, since at those energies Galactic magnetic field is not strong enough to isotropise UHECR trajectories. Region between knee and ankle is transition region. Position of second ankle at energy approximately 26 times higher as compared to knee energy suggests that it's origin is due to contribution of Galactic iron nuclei if knee dominated by protons.

Models of cosmic rays which explain observed spectrum are discussed in recent review [6].

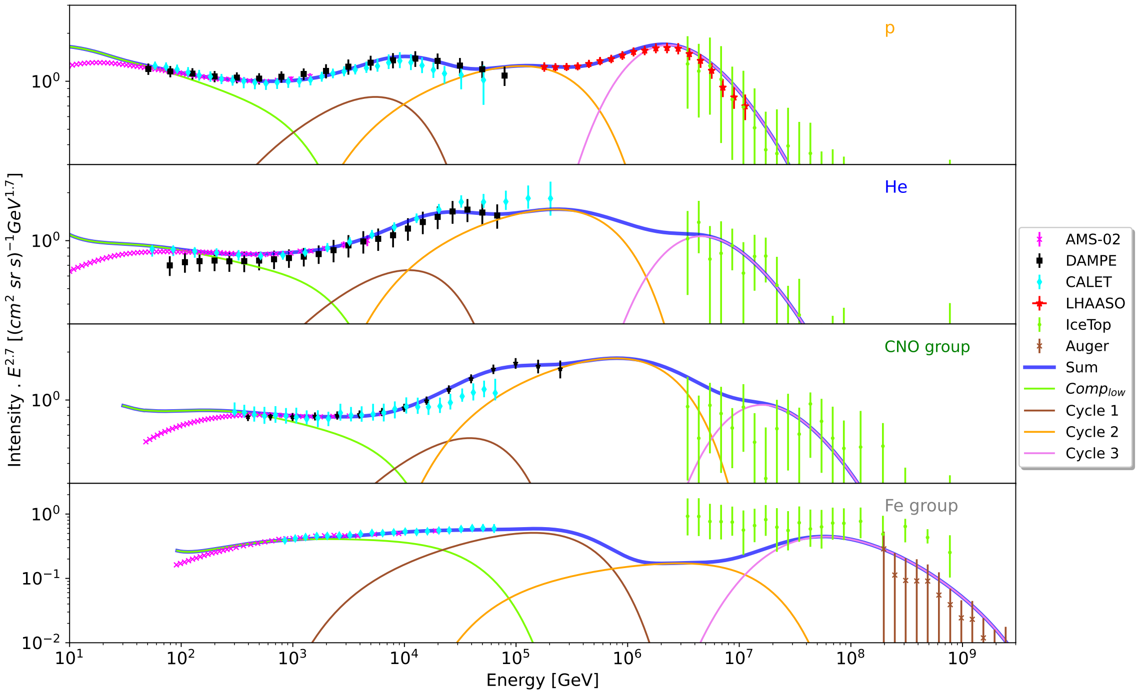

Figure 3: Cosmic ray spectra obtained for p, He, CNO and heavy elemental groups with Model A, composed of three Peters cycles and an additional low energy component. The data are from AMS-02 [7, 13–15], DAMPE [8, 16, 17], CALET [9, 18–20], LHAASO [5], IceTop [11] and Auger [12, 21].

Cosmic ray proton spectrum measured by AMS-02 [7], DAMPE[8], CALET[9], LHAASO[10], IceCube [11] and Auger[12] shown in the Fig. 2. Spectrum is multiplied by $E^{2.7}$ and stays almost constant from GeV to PeV energy, for which Galactic sources dominate cosmic ray signal. All features of total spectrum except second knee are clearly visible in the proton spectrum. One can see that spectrum below knee has complicated structure with 3 bumps.

In recent work [27] two models A and B was constructed to show range of possibilities to fit cosmic ray data up to knee region. Model A uses Peters cycles for modelling of Galactic CR population [28, 29]. The rigidity spectra of different elemental groups only differ in their relative normalisations[1]. The method is very similar to what is presented in Ref. [30]. For Model B account for spectral features in the local CR spectrum via spectral changes that arise from the diffusive propagation of CRs in the Galactic magnetic field. Five breaks in the power-law rigidity dependence of diffusion coefficient $D(\mathcal{R})$ was implemented adopted from Ref. [31]. This diffusion model was implemented into the DRAGON-2 code [32], which numerically solves the full CR transport equations.

Result CR spectrum fit with model A is presented in the Fig. 3 for p, He, CNO and heavy elemental groups. Same model fits total spectrum and $< logA >$ as shown in the Fig. 4.

So far we discussed measurements and their interpretation at Earth position. For long time it was assumed that cosmic rays are uniformly distributed in Galactic plane with some gradient

[1]This assumption is valid for primary CR nuclei in the energy range in which spallation reactions do not lead to significant changes in the spectrum on the time scale of residence of CRs in the Galaxy, which is true for $E > 1$ TeV.

PoS(ICRC2025)1399

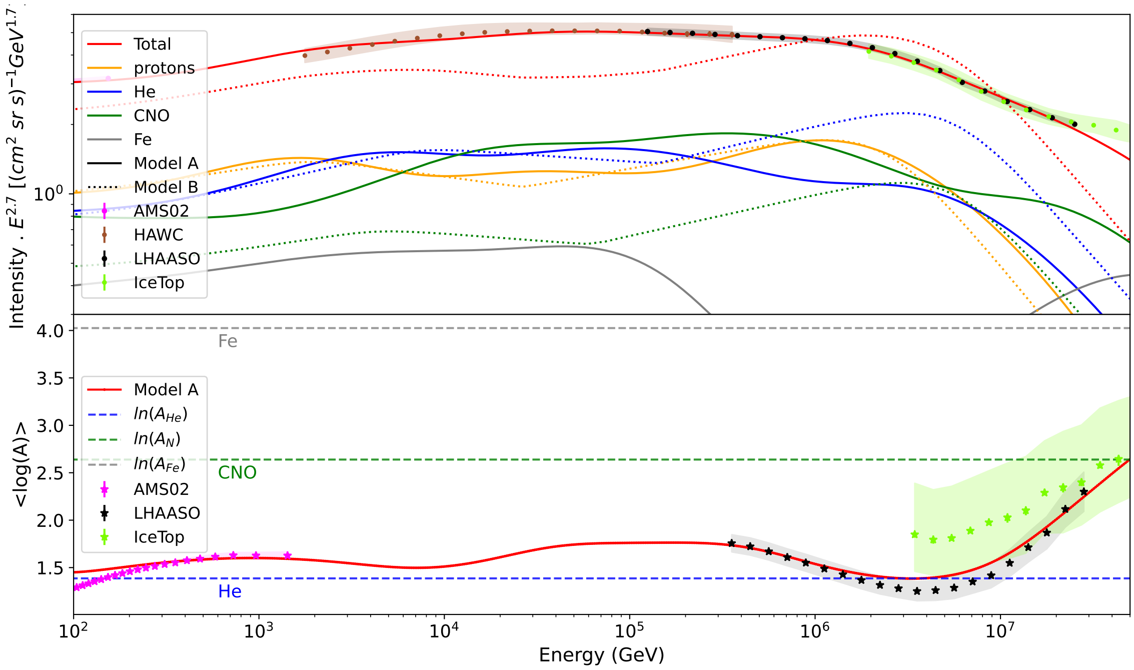

Figure 4: Result of the fit for the all-particles spectrum, and mean logarithmic mass of the CR spectrum with model A. The data are from AMS-02 [13–15, 22, 23], HAWC [24], LHAASO [25] and IceTop [26]. Only LHAASO's data points were used in the fit.

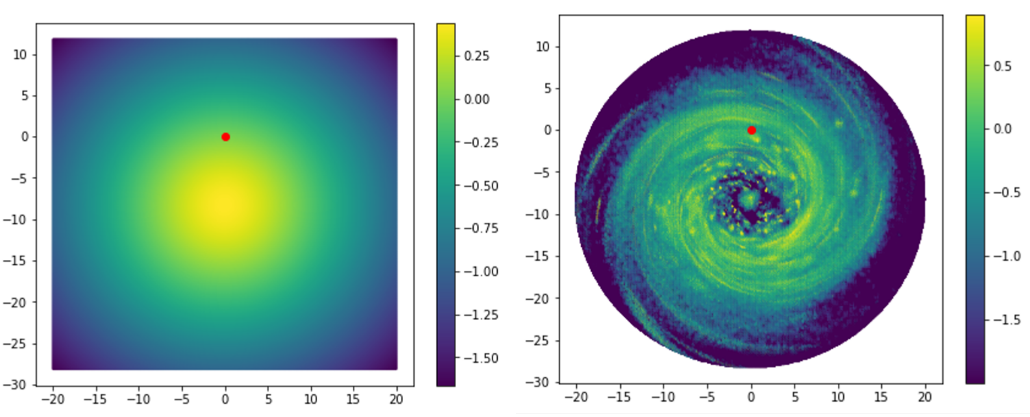

Figure 5: Left: PeV cosmic ray distribution in Galactic plane in axial-symmetric model. Right: PeV cosmic ray distribution in Galactic plane in 3-dimentional model. X and Y axis are in kpc units. Color show $log10$ density of cosmic rays normalized to 1 at Earth measurements. Earth position is shown with red dot at (0,0).

towards central Galaxy due to larger number of sources there. This approximation is true for large number of sources. At highest energies number of source is small, distribution of cosmic rays in Galaxy is inhomogeneous and contributions of individual sources is important at given point of Galaxy [33] . In Fig. 5 we show distribution of cosmic rays in Galactic plane in two cases. Left figure show axial-symmetric case of cosmic rays. At right figure is 3-dimensional distribution of cosmic rays from finite number of sources.

Number of contributing sources depends on lifetime of cosmic rays in Galaxy and in maximum energy to which they are able accelerate cosmic rays. At $E = 1$ GeV cosmic rays stay in Galaxy 30 Myr, taking into account 3 sources per century and that all CR source are able to accelerate to this energy we have 10^6 sources contributing to cosmic ray flux at any time, so approximation shown in the Fig. 5 left is valid. Contrary at $E = 1$ PeV lifetime of cosmic rays in Galaxy is 0.3 Myr and we have only 10^4 sources contributing to cosmic rays at the same time if all of them are able to accelerate to PeV energies. In Fig. 5 we see case when only 1.6% of sources are able to accelerate to PeV energies and number of contributing sources is around 150 in this figure, see details in ref. [33].

To conclude, local cosmic ray flux can be modelled by contributions of several populations of sources at different energy range. Gamma-ray and neutrino measurements, presented below additionally constrain this model and distinguish between two cases in the Fig. 5.

2. Diffused gamma rays from Galactic plane

Diffused gamma-rays in Milky Way Galaxy are produced by three main processes, pion production in cosmic ray nuclei interactions with interstellar gas and by inverse Compton scattering of background photons by cosmic ray electrons and bremsstrahlung process. Additional contributions to diffused background come from unresolved sources, both hadronic and leptonic. Note, that both distributions of electrons and cosmic rays in Galaxy is unknown a-priori. Distribution of interstellar gas is well known in two-dimensional sky map, measured by Planck, but its real three-dimensional structure has large uncertainties.

$$\begin{aligned} I_{\gamma,\nu}(E,l,b) &= \frac{c}{4\pi} \sum_{A,A'} \int_0^\infty ds\, n_{\rm gas}^A(x) e^{-\tau_\gamma(s,E)} \\ & \int_E^\infty dE' \, \frac{d\sigma^{A'A\to X\gamma,\nu}(E',E)}{dE} \frac{dN_{\rm CR}^{A'}}{dV\, dE'}, \end{aligned} \quad (1)$$

Pion production contribution to diffused gamma-ray and neutrino fluxes as function of energy E and galactic coordinates (l,b) is presented by Eq. (1).

Diffused Gamma-ray Emission (DGE) of Milky Way was measured in energy rage from 100 MeV to 100 GeV by Fermi LAT [34]. At TeV energy first lower bound on diffused gamma-ray flux was established by HESS in ref [35]. Later it was found extension of Fermi LAT diffused background up to TeV energy [36], which allowed to cover four orders of magnitude in energy measurement of diffused background with Fermi LAT. Recently diffused gamma-ray background was measured at higher energies from $E > 1$ TeV up to PeV energies by LHAASO [37, 38] for Northen sky. However this measurement can be considered as low limit in the inner Galaxy, since it

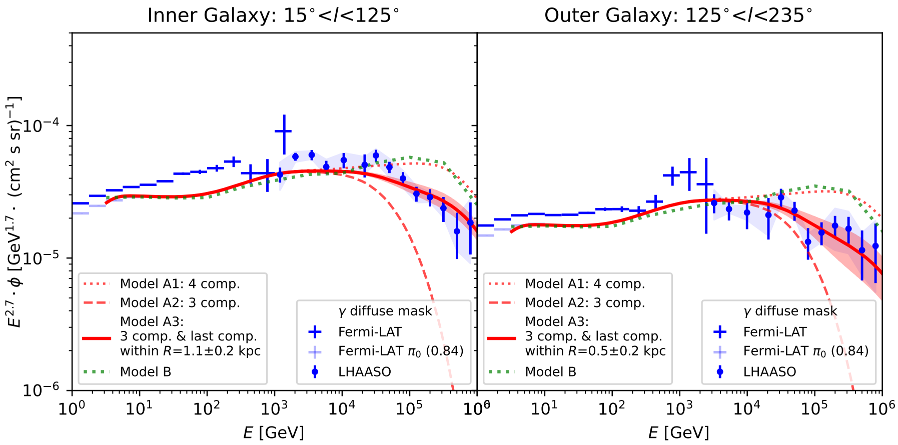

Figure 6: Contribution to the diffused gamma-ray background from cosmic ray models, which explain local cosmic ray measurements with several populations of sources from ref. [27].

does not include regions around LHAASO sources. In inner Galaxy this excludes most of Galactic plane, from which one expects most of DGE. Contrary, measurement of LHAASO in outer Galaxy is close to final one since there excluded sources does not cover large fraction of Galactic plane.

According to Fermi collaboration modelling of diffused flux, this emission dominated by hadronic contribution at 10 GeV, and it is about 85% of total DGE emission at 10 GeV [39].

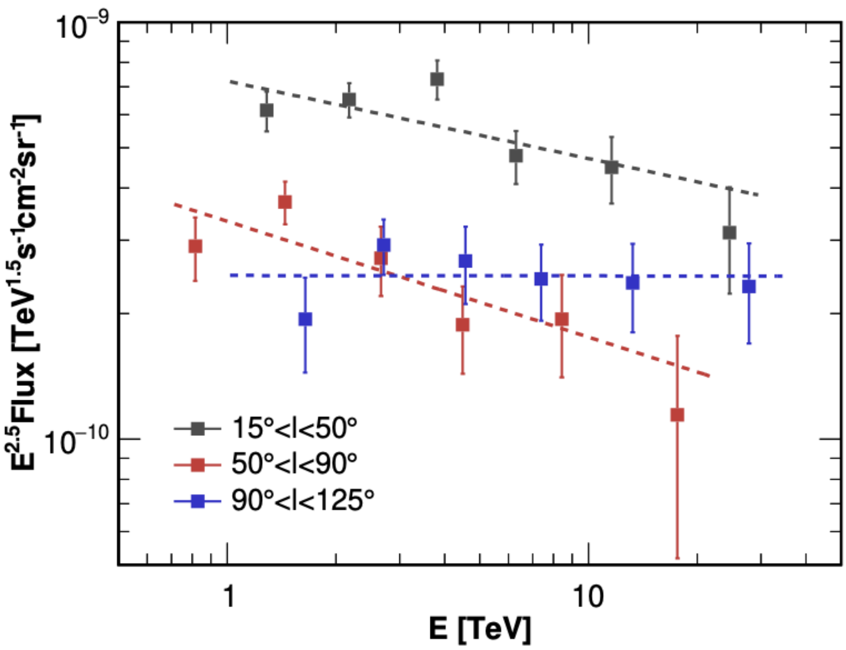

Figure 7: Diffused gamma-ray flux from several regions of Milky Way Galaxy measured by LHAASO [38].

For production of secondary gamma-rays and neutrinos we used AAFrag code [40, 41]. We used gas density models from ref. [42]. We modelled cosmic ray flux with models A for Peters circle model or model B with propagation breaks as discussed with previous section. Results of simulations from ref [27] are presented in the Fig. 6.

One can see in the Fig. 6 that both models A and B explain significant fraction of total diffused gamma-ray flux both in inner and outer Galaxy up to 100 TeV. However, in the knee region they predict too high gamma-ray flux well above LHAASO measurements. This can be first indication of finite number of sources in Galaxy at those high energies, see Fig. 5. In Fig. 6 we fitted observed LHAASo flux with contribution of CR up to 1.5 kpc in inner Galaxy and 0.7 kpc in outer Galaxy. This indicate that if we have finite number of osurces in Galaxy at those high energies, one of then should be around us, but this source should be relatively old in order we see CR up to 0.7 in outer Galaxy. Flux in inner Galaxy in this case have contribution both from this local source and from several other sources.

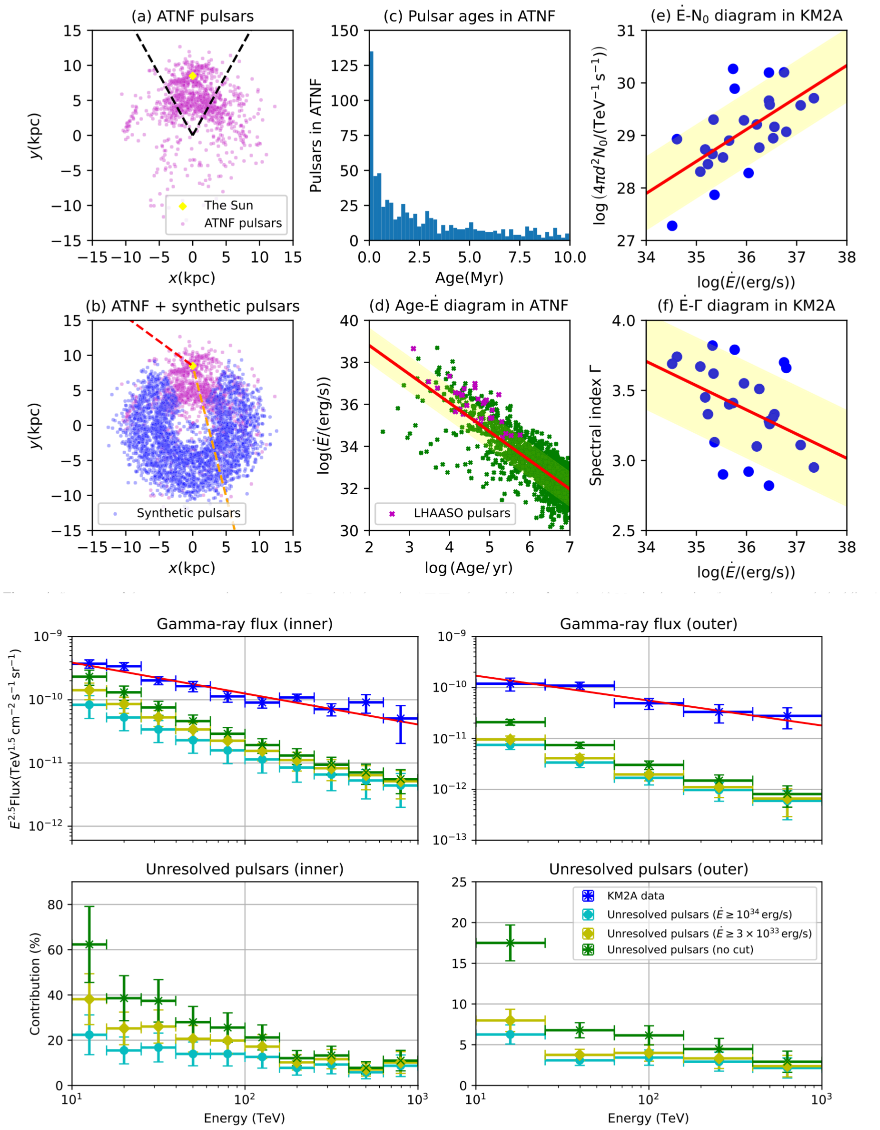

Figure 8: Contribution of unresolved PWN to galactic diffused emission froim ref [43].

Indication that simple models with same cosmic ray flux as measured at Earth are not working in Milky Way Galaxy was shown both by HAWC [44] and LHAASO [38]. In particular in the Fig. 7 we present diffused gamma-ray flux measured by LHAASO in several regions of Galaxy, where inner part of Galaxy was divided in three parts. From this figure one can see that cosmic rays in different parts of Galaxy not only have different flux, which can be explained by change in source density, but also have different spectrum, which can be indication of significant variation of cosmic ray flux over Galaxy and contribution of several populations of sources, differently distributed in Galaxy.

Most of sources in 1 LHAASO catalog are Pulsar Wind Nebulas (PWN) [45]. Those objects are leptonic sources, since they contain electrons and positrons emitted by pulsars for their lifetime. If major fraction of resolved sources are PWN, some unknown contribution of unresolved sources to diffused flux can potentially give significant contribution to the diffused gamma-ray background.

This contribution was studied in detail in ref. [43]. in the Fig. 8 we presented results of this study. Upper panels of this figure show how one can model PWN distribution in Galaxy. Low panels show contribution of unresolved pulsars to diffused gamma-ray background. Depending on assumptions of model, contribution of unresolved PWN is below 20 % in inner Galaxy and 10 % in outer Galaxy above 100 TeV. Recent more detailed study [46] show that this contribution is always below 30% up to TeV energies. This is consistent with models presented in the Fig. 6. Important discriminations of hadronic and leptonic contributions to the gamma-ray flux are neutrinos coming from Galaxy.

3. Neutrinos from Galactic plane

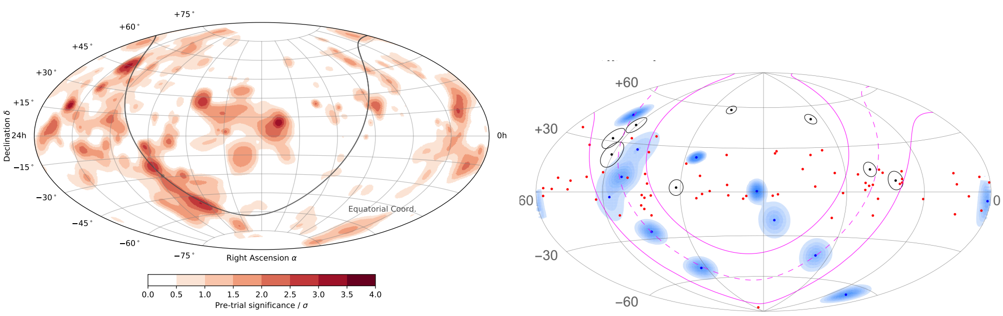

Figure 9: Left: Sky map of excesses above background of cascade events in IceCube [47]. Right: individual cascade events arrival directions with $E > 200$ TeV in IceCube and Baikal from ref [48].

Neutrino flux from the Milky Way Galaxy consist from contribution of flux of individual sources and neutrino diffused flux which is produced by cosmic ray interaction with interstellar gas. It was first predicted by Berezinsky and A.Smirnov in 1975 [50]. Already first data of IceCube have shown evidence of the neutrino flux from Galaxy [51, 52].

Very promising region of Galaxy is Galactic Ridge, central part of Galaxy with $|l| < 30°$. Cosmic ray models predict significant flux of neutrinos from this region due to both high gas density and large number of cosmic rays [6]. ANTARES collaboration in 2022 found 2-sigma hint of neutrino emission from galactic ridge [53]. Later in 2023 IceCube collaboration found 4

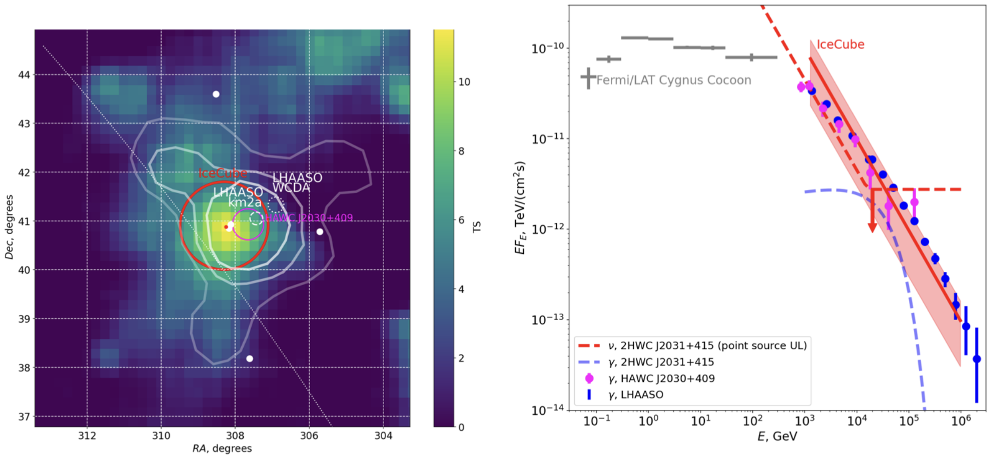

Figure 10: Left: Sky map of excesses above background of events in IceCube 10 years of data in direction to Cygnus region. Right: consistent gamma-ray and neutrino flux measurements of Cygnus cocoon from ref [49].

σ evidence of neutrino emission from Galaxy [47]. Significance of neutrino flux from different regions of sky measured by IceCube is shown in Fig. 9 on left panel. Most significant neutrino flux in this figure come from direction to Galactic Ridge. In recent study of ref. [54] it was shown that most of emission in Galactic Ridge should be of hadronic origin.

At highest energies Galaxy also significantly contribute to the neutrino flux. Sky map of high energy neutrino measurements with $E > 200$ TeV from [48] is shown in right panel. IceCube cascade events are presented with blue regions, while Baikal-GVD events are shown with black circles. In both cases significant fraction of diffuse flux come from direction to Galactic plane. According to ref. [48] combined IceCube and Baikal-GVD data show evidence of Galactic contribution to astrophysical neutrinos within 10 degrees from Galactic plane. Same figure show directions of cascade events of IceCube, which also show independent evidence of signal from Galactic plane [55]. High galactic latitude contributions required by study of [55] should be local. Such contributions to diffuse neutrino flux can come from cosmic ray interactions in Local Bubble and nearby sources [56].

Cygnus region is extended region of sky located around galactic plane at $l = 80$ degress was radius about 5 degrees. This region is part of Galactic arm, which we see in tangential direction and it contain both very high density of gas and large number of sources. Cygnus Cocoon within Cygnus region with hard spectrum was detected in first years of Fermi LAT data [57]. HAWC detected high energy gamma-rays from Cygnus cocoon in ref. [58]. Later LHAASO detected Cygnus cocoon even at higher energies $LHAASO\ J2027+4119$ [59].

Sky map of excesses above background of events in IceCube 10 years of data [60] in direction to Cygnus region is shown in Fig. 10 left panel. One can see excess in the direction of Cygnus cocoon on the level of 3 σ. Right panel show neutrino flux from this region from ref. [49], which is completely consistent with gamma-ray flux.

In Fig.11 we plot total gamma-ray flux measured by Fermi LAT and LHAASO in inner (left panel) and outer (right panel) Galaxy with black points. IceCube galactic flux was adapted from all

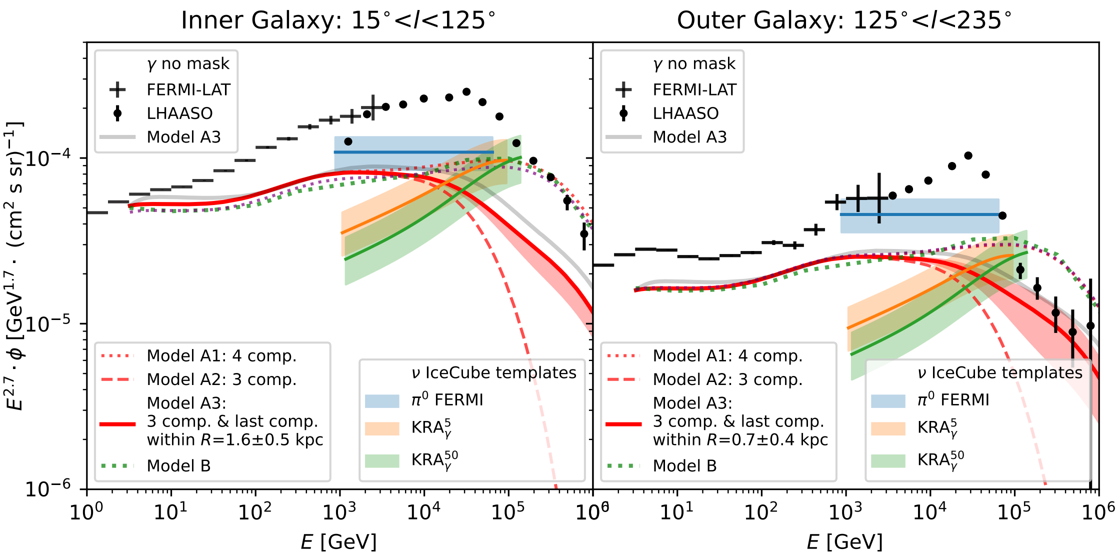

Figure 11: Total gamma-ray flux in inner and outer Galaxy measured by Fermi LAT and LHAASO as compared to IceCube neutrino spectrum from Galaxy normalised to those regions and to models of cosmic rays from ref. [27].

sky templates to LHAASO regions. At same figure we show predictions for diffuse neutrino flux from Galaxy from models A and B of ref [27]. One can see that model predictions are consistent with $1/E^{2.7}$ IceCube flux, still leaving place for some hadronic point source contribution both in inner and outer Galaxy.

4. Conclusions

In this talk I reviewed multi-messenger observations of Milky-Way Galaxy with cosmic rays, high energy gamma-rays and neutrinos.

The cosmic-ray fluxes of individual nuclei have been measured by satellite experiments. AMS-02, DAMPE, and CALET observe several spectral breaks that require explanation. LHAASO has, for the first time, measured the precise proton spectrum from the ground with small statistical and systematic uncertainties. The mass composition at the knee has been established with high-precision measurements of $< logA >$ and the total flux. As a next step, accurate measurements of the mass composition in the energy range from 10 PeV to 1 EeV are required. Breaks in the cosmic-ray proton spectrum from GeV to PeV energies may originate from propagation effects and from contributions of different populations of sources. Several models have been proposed to explain the existing cosmic-ray data. These models can be distinguished using gamma-ray and neutrino observations of the Milky Way.

We are beginning to understand the general structure of the magnetic field in the Milky Way. Cosmic-ray fluxes in different regions of the Galaxy can be studied using gamma-ray and neutrino observations. Diffuse gamma-ray emission from the Milky Way has been measured by Fermi-LAT at energies between 1 GeV and 1 TeV, and by LHAASO between 1 TeV and 1 PeV. Measurements of the Southern sky require SWGO. The first indications of neutrinos from the Galaxy have been observed in cascade events by IceCube, with hints also reported by ANTARES and Baikal-GVD; first results from KM3NeT are anticipated. Evidence for the first Galactic neutrino source, the Cygnus Cocoon, has been found, with its neutrino flux observed in ten years of IceCube data. However, the fraction of the neutrino signal originating from isolated sources remains uncertain. Next-generation neutrino telescopes—such as IceCube-Gen2, TRIDENT, and HUNT—are needed to disentangle contributions from individual sources and the diffuse Galactic neutrino background.

Acknowlegments

I would like to thank my collaborators Clément Prevotat and Sergey Koldobskiy for their kind help to prepare some figures of this talk.

References

[1] AMS collaboration, *The Alpha Magnetic Spectrometer (AMS) on the international space station: Part II — Results from the first seven years*, Phys. Rept. **894** (2021) 1.

[2] CALET collaboration, *Direct Measurement of the Cosmic-Ray Helium Spectrum from 40 GeV to 250 TeV with the Calorimetric Electron Telescope on the International Space Station*, Phys. Rev. Lett. **130** (2023) 171002 [2304.14699].

[3] DAMPE collaboration, *Measurement of the cosmic-ray proton spectrum from 40 GeV to 100 TeV with the DAMPE satellite*, Sci. Adv. **5** (2019) eaax3793 [1909.12860].

[4] G.V. Kulikov and G.B. Khristiansen, *On the Size Spectrum of Extensive Air Showers*, *JETP* **8** (1959) 441.

[5] LHAASO collaboration, *Measurements of All-Particle Energy Spectrum and Mean Logarithmic Mass of Cosmic Rays from 0.3 to 30 PeV with LHAASO-KM2A*, Phys. Rev. Lett. **132** (2024) 131002 [2403.10010].

[6] M. Kachelriess and D.V. Semikoz, *Cosmic Ray Models*, Prog. Part. Nucl. Phys. **109** (2019) 103710 [1904.08160].

[7] M. Aguilar, L.A. Cavasonza et al., *The Alpha Magnetic Spectrometer (AMS) on the international space station: Part II - Results from the first seven years*, Physics Reports **894** (2021) .

[8] Q. An, R. Asfandiyarov et al., *Measurement of the cosmic ray proton spectrum from 40 GeV to 100 TeV with the DAMPE satellite*, Science Advances **5** (2019) .

[9] O. Adriani, Y. Akaike, K. Asano, Y. Asaoka, E. Berti, G. Bigongiari et al., *Observation of Spectral Structures in the Flux of Cosmic-Ray Protons from 50 GeV to 60 TeV with the Calorimetric Electron Telescope on the International Space Station*, Phys.Rev.Lett. **129** (2022) 101102 [2209.01302].

[10] LHAASO collaboration, *First Identification and Precise Spectral Measurement of the Proton Component in the Cosmic-Ray 'Knee'*, 2505.14447.

[11] M.G. Aartsen, M. Ackermann, J. Adams, J.A. Aguilar, M. Ahlers, M. Ahrens et al., *Cosmic ray spectrum and composition from PeV to EeV using 3 years of data from IceTop and IceCube*, *Physical Review D* **100** (2019) 82002 [1906.04317].

[12] P.A. Abdul Halim et al., *Highlights from the pierre auger observatory*, *PoS* **ICRC2023** (2023) 016.

[13] M. Aguilar, L.A. Cavasonza et al., *Properties of Cosmic-Ray Sulfur and Determination of the Composition of Primary Cosmic-Ray Carbon, Neon, Magnesium, and Sulfur: Ten-Year Results from the Alpha Magnetic Spectrometer*, *Phys.Rev.Lett.* **130** (2023) .

[14] M. Aguilar, L. Ali Cavasonza, G. Ambrosi, L. Arruda, N. Attig, A. Bachlechner et al., *Properties of Cosmic Helium Isotopes Measured by the Alpha Magnetic Spectrometer*, *Phys.Rev.Lett.* **123** (2019) 181102.

[15] M. Aguilar, L. Cavasonza et al., *Properties of Iron Primary Cosmic Rays: Results from the Alpha Magnetic Spectrometer*, *Phys.Rev.Lett.* **126** (2021) .

[16] DAMPE collaboration, *DArk Matter Particle Explorer: 7 years in Space*, *PoS* **ICRC2023** (2024) 003.

[17] F. Alemanno, Q. An et al., *Measurement of the Cosmic Ray Helium Energy Spectrum from 70 GeV to 80 TeV with the DAMPE Space Mission*, *Phys.Rev.Lett.* **126** (2021) .

[18] O. Adriani, Y. Akaike, K. Asano, Y. Asaoka, E. Berti, G. Bigongiari et al., *Direct Measurement of the Cosmic-Ray Helium Spectrum from 40 GeV to 250 TeV with the Calorimetric Electron Telescope on the International Space Station*, *Phys.Rev.Lett.* **130** (2023) 171002 [2304.14699].

[19] P.S. Marrocchesi, O. Adriani, Y. Akaike, Y. Asaoka, E. Berti, G. Bigongiari et al., *CALET Observations during the First 5 Years on the ISS*, *Physics of Atomic Nuclei* **84** (2021) 985.

[20] O. Adriani, Y. Akaike, K. Asano, Y. Asaoka, E. Berti, G. Bigongiari et al., *Measurement of the Iron Spectrum in Cosmic Rays from 10 GeV /n to 2.0 TeV /n with the Calorimetric Electron Telescope on the International Space Station*, *Phys.Rev.Lett.* **126** (2021) 241101 [2106.08036].

[21] P. Abreu, M. Aglietta et al., *The energy spectrum of cosmic rays beyond the turn-down around* 10^{17} *ev as measured with the surface detector of the pierre auger observatory*, *The European Physical Journal C* **81** (2021) .

[22] AMS Collaboration collaboration, *Precision measurement of the proton flux in primary cosmic rays from rigidity 1 gv to 1.8 tv with the alpha magnetic spectrometer on the international space station*, *Phys. Rev. Lett.* **114** (2015) 171103.

[23] AMS Collaboration collaboration, *Observation of the identical rigidity dependence of he, c, and o cosmic rays at high rigidities by the alpha magnetic spectrometer on the international space station*, *Phys. Rev. Lett.* **119** (2017) 251101.

[24] J.A. Morales-Soto, J.C. Arteaga-Velázquez, Hawc, A.U. Abeysekara, A. Albert, R. Alfaro et al., *The all-particle cosmic ray energy spectrum measured with HAWC*, in *37th International Cosmic Ray Conference*, p. 330, Mar., 2022, DOI [2108.04748].

[25] LHAASO collaboration, *Measurement of Ultra-High-Energy Diffuse Gamma-Ray Emission of the Galactic Plane from 10 TeV to 1 PeV with LHAASO-KM2A*, *Phys. Rev. Lett.* **131** (2023) 151001 [2305.05372].

[26] M.G. Aartsen, M. Ackermann et al., *Cosmic ray spectrum and composition from pev to eev using 3 years of data from icetop and icecube*, *Physical Review D* **100** (2019) .

[27] C. Prevotat, Z. Zhu, S. Koldobskiy, A. Neronov, D. Semikoz and M. Ahlers, *Diffuse gamma-ray and neutrino emission from the Milky Way and the local knee in the cosmic ray spectrum*, 2507.10823.

[28] B. Peters, *Primary Cosmic Radiation and Extensive Air Showers*, *Nuovo Cim.* **22** (1961) 800.

[29] G. Zatsepin, N. Gorunov and L. Dedenko*Izv. Akad. Nauk USSR Ser. Fiz.* **26** (1962) 685.

[30] C. Prevotat, M. Kachelriess, S. Koldobskiy, A. Neronov and D. Semikoz, *Energy dependence of the knee in the cosmic-ray spectrum across the Milky Way*, *Phys. Rev. D* **110** (2024) 103035 [2407.11911].

[31] G. Schwefer, P. Mertsch and C. Wiebusch, *Diffuse emission of galactic high-energy neutrinos from a global fit of cosmic rays*, *The Astrophysical Journal* **949** (2023) 16.

[32] C. Evoli, D. Gaggero, A. Vittino, G.D. Bernardo, M.D. Mauro, A. Ligorini et al., *Cosmic-ray propagation with dragon2: I. numerical solver and astrophysical ingredients*, *Journal of Cosmology and Astroparticle Physics* **2017** (2017) 015.

[33] G. Giacinti and D. Semikoz, *Model of Cosmic Ray Propagation in the Milky Way at the Knee*, 2305.10251.

[34] Fermi-LAT collaboration, *Fermi-LAT Observations of the Diffuse Gamma-Ray Emission: Implications for Cosmic Rays and the Interstellar Medium*, *Astrophys. J.* **750** (2012) 3 [1202.4039].

[35] H.E.S.S. collaboration, *Diffuse Galactic gamma-ray emission with H.E.S.S*, *Phys. Rev. D* **90** (2014) 122007 [1411.7568].

[36] A. Neronov and D. Semikoz, *Galactic diffuse gamma-ray emission at TeV energy*, *Astron. Astrophys.* **633** (2020) A94 [1907.06061].

[37] LHAASO collaboration, *Measurement of ultra-high-energy diffuse gamma-ray emission of the galactic plane from 10 tev to 1 pev with lhaaso-km2a*, *Phys. Rev. Lett.* **131** (2023) 151001 [2305.05372].

[38] L. collaboration, *Measurement of Very-High-Energy Diffuse Gamma-Ray Emissions from the Galactic Plane with LHAASO-WCDA*, *Physical Review Letters* **134** (2025) 81002.

[39] Fermi-LAT collaboration, *Development of the Model of Galactic Interstellar Emission for Standard Point-Source Analysis of Fermi Large Area Telescope Data*, *Astrophys. J. Suppl.* **223** (2016) 26 [1602.07246].

[40] M. Kachelrieß, I.V. Moskalenko and S. Ostapchenko, *AAfrag: Interpolation routines for Monte Carlo results on secondary production in proton–proton, proton–nucleus and nucleus–nucleus interactions*, *Computer Physics Communications* **245** (2019) 106846 [1904.05129].

[41] S. Koldobskiy, M. Kachelrieß, A. Lskavyan, A. Neronov, S. Ostapchenko and D.V. Semikoz, *Energy spectra of secondaries in proton-proton interactions*, *Phys.Rev. D* **104** (2021) 123027 [2110.00496].

[42] P. Lipari and S. Vernetto, *Diffuse Galactic gamma ray flux at very high energy*, *Phys. Rev. D* **98** (2018) 043003 [1804.10116].

[43] S. Kaci, G. Giacinti and D. Semikoz, *On the Contribution of Unresolved Pulsars to the Ultra-high-energy Galactic Diffuse Gamma-Ray Emission*, *Astrophys. J.* **975** (2024) L6 [2407.20186].

[44] HAWC collaboration, *Galactic Gamma-Ray Diffuse Emission at TeV Energies with HAWC Data*, *Astrophys. J.* **961** (2024) 104 [2310.09117].

[45] LHAASO collaboration, *The First LHAASO Catalog of Gamma-Ray Sources*, *Astrophys. J. Suppl.* **271** (2024) 25 [2305.17030].

[46] S. Kaci, G. Giacinti and D. Semikoz, *A Self-Consistent Model of the Ultra High-Energy Gamma-Ray Emission of Pulsar Wind Nebulae: Insights from LHAASO and ATNF Catalogs*, 2511.20452.

[47] IceCube collaboration, *Observation of high-energy neutrinos from the Galactic plane*, *Science* **380** (2023) adc9818 [2307.04427].

[48] Baikal-GVD collaboration, *Probing the Galactic Neutrino Flux at Neutrino Energies above 200 TeV with the Baikal Gigaton Volume Detector*, *Astrophys. J.* **982** (2025) 73 [2411.05608].

[49] A. Neronov, D. Semikoz and D. Savchenko, *Neutrino signal from Cygnus region of the Milky Way*, *Phys. Rev. D* **110** (2024) 043024 [2311.13711].

[50] V.S. Berezinsky and A.Y. Smirnov, *Cosmic neutrinos of ultra-high energies and detection possibility*, *Astrophys. Space Sci.* **32** (1975) 461.

PoS(ICRC2025)1399

[51] A. Neronov, D.V. Semikoz and C. Tchernin, *PeV neutrinos from interactions of cosmic rays with the interstellar medium in the Galaxy*, *Phys. Rev. D* **89** (2014) 103002 [1307.2158].

[52] A. Neronov and D.V. Semikoz, *Evidence the Galactic contribution to the IceCube astrophysical neutrino flux*, *Astropart. Phys.* **75** (2016) 60 [1509.03522].

[53] ANTARES collaboration, *Hint for a TeV neutrino emission from the Galactic Ridge with ANTARES*, *Phys. Lett. B* **841** (2023) 137951 [2212.11876].

[54] A. Neronov, D. Semikoz, J. Aublin, M. Lamoureux and A. Kouchner, *Hadronic nature of high-energy emission from the Galactic ridge*, *Phys. Rev. D* **108** (2023) 103044 [2307.07978].

[55] Y.Y. Kovalev, A.V. Plavin and S.V. Troitsky, *Galactic Contribution to the High-energy Neutrino Flux Found in Track-like IceCube Events*, *Astrophys. J. Lett.* **940** (2022) L41 [2208.08423].

[56] M. Bouyahiaoui, M. Kachelrieß and D. Semikoz, *Hot spots in the neutrino flux created by cosmic rays from Cygnus and Vela*, *Phys. Rev. D* **106** (2022) 063004 [2105.13378].

[57] M. Ackermann et al., *A Cocoon of Freshly Accelerated Cosmic Rays Detected by Fermi in the Cygnus Superbubble*, *Science* **334** (2011) 1103.

[58] A.U. Abeysekara et al., *HAWC observations of the acceleration of very-high-energy cosmic rays in the Cygnus Cocoon*, *Nature Astron.* **5** (2021) 465 [2103.06820].

[59] LHAASO collaboration, *An ultrahigh-energy γ-ray bubble powered by a super PeVatron*, *Sci. Bull.* **69** (2024) 449 [2310.10100].

[60] IceCube collaboration, *IceCube Data for Neutrino Point-Source Searches Years 2008-2018*, 2101.09836.

....